25th ABCM International Congress of Mechanical Engineering
October 20-25, 2019, Uberlândia, MG, Brazil

COB-2019-0752
AMPLITUDE AND FREQUENCY RESPONSES OF A TWO-DEGREE-OF-FREEDOM CYLINDER APPLIED TO FLUID FLOW

Matheus Rover Barbieri
Jonathan Utzig
Henry França Meier
Chemical Engineering Department, University of Blumenau
São Paulo St., 3250, I-303 – 89030-000 Blumenau – Santa Catarina - Brazil
matheus_rover@hotmail.com
jutzig@furb.br
meier@furb.br

Abstract. *The study of the crossflow over bluff bodies has received special attention throughout the years, motivated by the occurrence of noise and damage in industrial applications. The presence of a cylinder modifies the flow around it, so that depending on flow velocity, vortex streets are formed downstream the tube. The motion amplitude and oscillation frequency are associated with these vortices patterns, in a way that the cylinder response depends on some factors such as the mass of the oscillating system and Reynolds number. An experimental methodology was proposed to investigate flow-induced vibrations, where a cylinder with a mass ratio equal to 13.66 was subject to crossflow with water as working fluid. The tube was suspended by four springs on a structure over the experimental facility, allowing it to oscillate with two degrees of freedom. Acceleration data were acquired in order to obtain motion amplitude and vibration frequency responses. The oscillation performance of the cylinder constituted an initial excitation branch and an upper branch, due to the applied velocity range, with amplitudes up to 1.3 diameters. The vibration frequency showed a dominant peak obtained through Fast Fourier Transform close to the natural frequency, resulting in a reduced frequency close to unity.*

Keywords: *flow-induced vibration, degrees of freedom, fluid-structure interaction, accelerometry.*

1. INTRODUCTION

There are several engineering situations in which flow-induced vibrations (FIV) are observed, which occur due to the two-way interaction between the fluid forces and the equipment surface reaction. This interaction depends on many factors, such as natural frequency (f_n), damping ratio (ζ), Reynolds number (*Re*) and mass ratio (m^*), which can cause tube vibration (Khalak and Williamson, 1997; Bearman, 2011). These vibrations are a possible source of damage to industries, once when they reach the natural vibration frequency of the structure, they intensify noise occurrence and amplitude of oscillation. This condition can risk the worker's security and the structural integrity of the equipment, leading to, in extreme cases, the structure's collapse. This phenomenon can reach many types of equipment such as heat exchangers and steam generators, in a way that the knowledge about forces associated with the flow over structures is of great importance for their design and fluid dynamic control (Blevins, 1990; Goyder, 2002).

The presence of a bluff body modifies the flow around it, due to the transient behavior of the fluid dynamic forces. The formation of vortex streets is associated with tube motion at a proper frequency, proportional to the flow velocity. In situations that the oscillation frequency gets closer to the natural frequency of the cylinder, a phenomenon called lock-in occurs, where the tube motion is correlated to the vortex street oscillation, controlling the instability mechanism that produces vortices shedding (Blevins, 1990). The effect of this is connected to an increase of the oscillation amplitude and the similarity between the natural vibration frequency and vortex shedding frequency, which is controlled by the cylinder oscillation (Norberg, 2003).

The vortices patterns are associated with the motion amplitude and oscillation frequency of the cylinder. Williamson and Roshko (1988) organized a chart relating different patterns to amplitudes of vibration and flow velocities. From all patterns, the most commonly encountered are 2S and 2P. The 2S pattern consists on the shed of one single vortex each half-cycle of oscillation, which is advected to the vortex street, as in the natural von Karman vortex shedding. The 2P pattern denotes the formation of a pair of vortices each half-cycle of oscillation. As an effect of these different vortex shedding patterns, alteration in the motion amplitude is expected, which are related to the branches of maximum vibration amplitude (Khalak and Williamson, 1999).

The mass ratio of an oscillating body is an important parameter concerning the analysis of flow-induced vibration, which is defined as the ratio between the mass of the oscillating system and the displaced fluid mass, according to Eq. 1:

$$m^* = \frac{4m}{\rho \pi D^2 L}, \tag{1}$$

where m is the mass of the oscillating system, D is the cylinder diameter, L is the cylinder length and ρ is the fluid density.

A cylinder with small mass ratio and free to oscillate only in the transversal direction experience three branches: an initial branch at low velocities, where the synchronization process starts and the motion is characterized by an increasing ramp of oscillation amplitude, with a 2S vortex pattern; increasing flow velocity, the motion reaches an upper branch, with greater amplitudes and the change to a 2P pattern, where the maximum displacements are observed; and increasing continuously the velocity, the amplitudes reduce to an inferior branch, but the vortex pattern is maintained. However, when the mass ratio is higher, characteristic of experiments conducted in less dense fluids, such as air, smaller maximum amplitudes are expected and the cylinder develops only the initial and inferior branches (Jauvtis and Williamson, 2004; Williamson and Govardhan, 2008).

The various response branches are associated with the reduced frequency (f^*), defined as the ratio between the oscillation frequency f and the cylinder natural frequency f_n, according to Eq. 2:

$$f^* = \frac{f}{f_n}. \tag{2}$$

Reaching the lock-in region, the frequency of vortex shedding becomes closer to the cylinder oscillation frequency, which maintains itself close to the natural vibration frequency, keeping f^* close to the unity. This baseline of constant f^* depends on the mass ratio, reaching higher values according to the decrease in the mass ratio.

An oscillating bluff body puts on movement a surrounding mass of fluid. In dense fluids, such as water, the effect of the displaced mass is considered through an added mass coefficient, which impacts the natural frequency (Blevins, 1990). Vikestad et al. (2000) conducted a study about the effects of added mass in a small mass ratio riser ($m^* = 1.30$). The authors observed that response frequencies depend on both the natural frequency and the added mass distribution over the structure. The added mass coefficient is dependent on the reduced velocity, defined in Eq. 3, presenting higher values in smaller reduced velocities and reaching a value of zero or even negative values according to the increase in the velocity:

$$U^* = \frac{U_{in}}{f_n D}, \tag{3}$$

where U_{in} is the channel inlet velocity.

Although most analyses are made considering only one degree of freedom in the transversal direction, previous studies have shown that adding a degree of freedom in the inline direction can indeed modify the crossflow response. Jauvtis and Williamson (2004) noted a great change in the fluid-structure interactions when mass ratios were reduced below 6. An amplification of the crossflow vibration in the upper branch, called the super-upper branch, yields amplitudes up to 1.5D. The inline motion amplitudes are close to 0.3D. This behavior led to a new periodic vortex-shedding mode, where a triplet of vortices is formed each half-cycle of oscillation.

The present work composes a broader study conducted by the research group at LFC/LVV – FURB, whose objective is the study of flow-induced vibration motivated mainly by industrial applications. In this context Silva et al. (2016) conducted a CFD-based design of experiments in tube bundles with water as working fluid, considering four transversal and longitudinal spacings between cylinders. Through the evaluation of flow patterns and force coefficients statistics, the authors emphasized the importance of considering different spacings between tubes once they lead to different effects over the response variables.

Silva et al. (2018) experimentally investigated flow patterns in four bundles varying the transversal and longitudinal spacings between the cylinders. By means of a Laser Doppler Anemometry technique, a bistable biased regime was observed in cylinder arrays with small transversal spacing, causing multiple Strouhal numbers. Silva et al. (2019) carried out a Large Eddy Simulation aiming to validate flow patterns and velocity profiles obtained in Silva et al. (2018). A correction in the classification of in-line arrangements was proposed, based on transversal and longitudinal spacings range, besides the evaluation of force coefficients acting over each cylinder.

Aiming to extend the study of flow-induced vibrations to other fluids, Barbieri et al. (2018) conducted numerical simulations of the crossflow over cylinder arrays with air as working fluid. The bundles had their transversal and longitudinal spacings between tubes varied according to experimental design, analyzing flow patterns and force coefficients statistics. Comparing the results with those from Silva et al. (2016), the change of the working fluid from water to air resulted in weaker force coefficients considering the same spacings between tubes. However, the presence of two more cylinders in each row of some arrays led to an increased mean drag coefficient and fluctuation of the lift force, even with a less dense fluid.

Accordingly, the present study aims to investigate the response variables of a two-degree-of-freedom cylinder, with a mass ratio equal to 13.66 and subject to crossflow with water as working fluid. Acceleration data are acquired with an accelerometer for further numerical integration and Fast Fourier Transform, obtaining, respectively, the amplitude of oscillation and the frequency of vibration responses.

2. MATERIALS AND METHODS

To achieve the objectives, an experimental methodology is proposed considering an accelerometer for acceleration data acquisition, a circular cylinder and an experimental facility built in acrylic, in a way that water enters in the base of the right reservoir, represented in Figure 1 by number (1). To reduce non-homogeneities in the incident flow a grid is placed at this reservoir outlet. Then, the water flows through the channel (2) and drains out to the outlet reservoir (3), at left, leaving the facility. The channel is 1 m long and 8 cm wide. The height of the channel is determined using support plates, set as 10.5 cm from its bottom. The channel is divided into three sections in such a way that the first and the third sections have support plates, while in the middle one the plates are absent, allowing the cylinder to vibrate. The cylinder has a diameter D = 1 cm and a submerged length L = 10.5 cm. It consists of an aluminum tube that does not charter, only translate, for the evaluation of its movement in both aligned and transversal directions to the flow. A 2D scheme of the single flexible cylinder inside the channel can be seen in Figure 2(a). The mass ratio (m^*) is equal to 13.66.

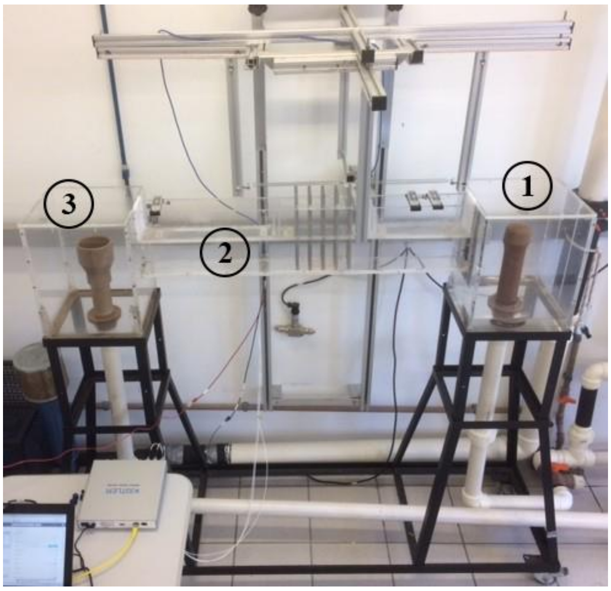

Figure 1. Flow-induced vibration experimental facility.

The tube must be suspended with no contact with any wall, once it can damp or suppress the vibration. This way, it is screw mounted to a K-Beam® triaxial accelerometer from Kistler SA, according to Figure 2(b), and this coupled system is attached to an independent support from the experimental facility, which is fixed at the laboratory wall, as can be seen in Figure 1. The group cylinder-accelerometer is suspended by a nylon wire, connected vertically at the support and four horizontal tension springs, two in each direction. The springs are responsible for supporting the group cylinder-accelerometer and reposition it in its initial position after each perturbation, granting characteristics such as natural frequency and damping ratio.

The water flow rate in the experimental facility is controlled through a program written in LabView (National Instruments SA). The data acquisition device (National Instruments SA, model USB-6211, maximum sampling rate capacity of 250 kHz at 16 bits) receives the pressure drop signal measured with a Venturi flowmeter coupled to a differential pressure transmitter. A PID algorithm sends a new signal to the frequency converter thereby controlling the rotational speed of the water pump. The pressure transmitter was calibrated before each experiment.

In this work, two sets of springs are used, each one consisting of four springs, once the cylinder has two degrees of freedom. Two springs are used in the transversal direction and the others in the longitudinal direction. They had their stiffness constants (k_{spring}) determined by Hooke's law, where the force applied in the spring is proportional to its displacement, through Eq. 4:

$$F = k_{spring} d, \tag{4}$$

where F is the force applied to the spring, k_{spring} is the stiffness constant and d is the displacement. Though, through a linear fit between the force and the displacement, the angular coefficient is equal to the stiffness constant. The constants obtained for the springs used in the present work are presented in Table **1**. Two groups of springs are used, with different stiffness constants, named set k5 for the weakest springs and set k92 for the strongest springs.

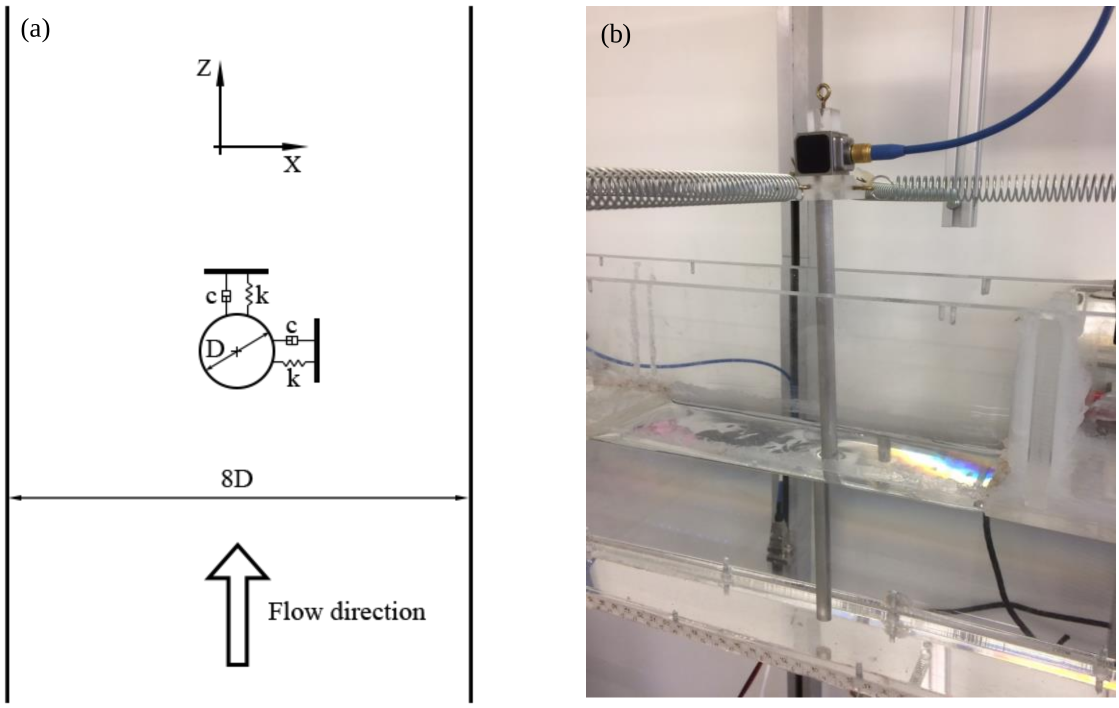

Figure 2. (a) 2D-scheme of the flow past a single flexible cylinder and (b) screw-mounted cylinder to the accelerometer.

Table 1. Stiffness constants for both sets of springs.

Spring set k5				Spring set k92			
Spring 1	Spring 2	Spring 3	Spring 4	Spring 1	Spring 2	Spring 3	Spring 4
3.77 N/m	5.94 N/m	3.95 N/m	5.84 N/m	92.01 N/m	91.02 N/m	90.65 N/m	90.15 N/m

In the study of flow-induced vibrations with cylinders free to oscillate, some parameters need to be determined to characterize the studied system, such as the natural frequency (f_n) and damping ratio (ζ). Both parameters can be obtained through free decay test, where a known displacement is imposed to the cylinder, normally equal to one diameter. Then, the tube is released until it becomes static again. Simultaneously, acceleration data are acquired and as in this work the cylinder moves with two degree-of-freedom, this procedure is conducted in both directions.

Applying a Fast Fourier Transform algorithm written in GNU Octave version 4.2.1 over the acceleration data, the natural frequency of the cylinder-accelerometer system adopted in the present work corresponds to the frequency with the higher energy in the power density spectrum. The damping ratio can be obtained through an exponential fit to the envelope of the acceleration data in the free decay test, where the maximum and minimum points are fitted to an exponential function corresponding to a sub damped system in a free-damped vibration, according to Eq. 5:

$$x = X \exp\left(-2\pi f_n \zeta t\right), \tag{5}$$

where x corresponds to the signal emitted by the accelerometer, X is a pre-exponential parameter and t is the time. This procedure resulted in natural frequencies and damping ratios obtained for both springs sets in each direction, whose values can be observed in Table **2**.

Table 2. Natural frequencies for the spring sets.

Natural frequency (Hz)				Damping ratio			
Spring set k92		Spring set k5		Spring set k92		Spring set k5	
Transversal	Longitudinal	Transversal	Longitudinal	Transversal	Longitudinal	Transversal	Longitudinal
8.8682	9.0610	3.1201	3.6733	0.0066	0.0059	0.1446	0.1652

At least three runs were conducted for all flow velocity conditions, to assure experimental reproducibility. For each velocity, data were acquired by five minutes with a sampling rate of 6250 Hz. After the Fourier Transform of the acceleration data, the mean dominant frequency was determined as well as its fluctuation. The inlet velocity (U_{in}) was varied between 0.1 and 0.3 m/s, corresponding to a reduced velocity (U^*) defined by Eq. 3 between approximately 1.1 and 3.5 for spring set k92 and between 3.3 and 10.0 for spring set k5.

3. RESULTS AND DISCUSSION

A single cylinder is subject to crossflow with water as working fluid in order to investigate the oscillation frequencies developed by the tube as well as the motion amplitude. The results contain frequency responses in both in the transversal and longitudinal directions to the flow, with both spring sets. The results related to the motion amplitude contains oscillation responses only in the transversal direction.

3.1 Evaluation of the oscillation frequencies

The vibration frequencies are shown in Figure 3(a) for spring set k92 and Figure 3(b) for spring set k5. The markers represent the mean of the triplicate obtained via Fast Fourier Transform while the bar of each marker represents the standard deviation, whose values are smaller than 2%, evidencing the reproducibility of the obtained results. One can also note in Figure 3(a) and (b) two straight lines: one line represents a constant frequency equal to the natural frequency, while the other represents frequencies related to a Strouhal number equal to 0.20, which is characteristic of the vortex shedding in the Reynolds regime practiced at the present work.

The spring set k5, whose main parameters are listed in Table **2**, produces a mass-damping parameter equal to 2.1159 and a velocity range corresponding to a reduced velocity between 3.17 and 10.18. The vibration frequency f shows values between 2.66 and 3.47 Hz for both transversal and longitudinal directions, corresponding to a reduced frequency f^* between 0.85 and 0.91, which demonstrates a coupled performance between the directions. The parameters for spring set k92 can also be seen in Table **2**, in a way that the group cylinder-accelerometer presents a mass-damping parameter equal to 0.085 and a reduced velocity ranging among 1.22 and 3.58. The reduced frequency presented values closer to unity, between 0.96 and 1.01, which corresponds to an oscillation frequency between 8.65 and 9.21 Hz, performing also similar values in both directions. In general, both springs sets developed a nearly constant reduced frequency baseline, although the values obtained with spring set k92 were closer to unity.

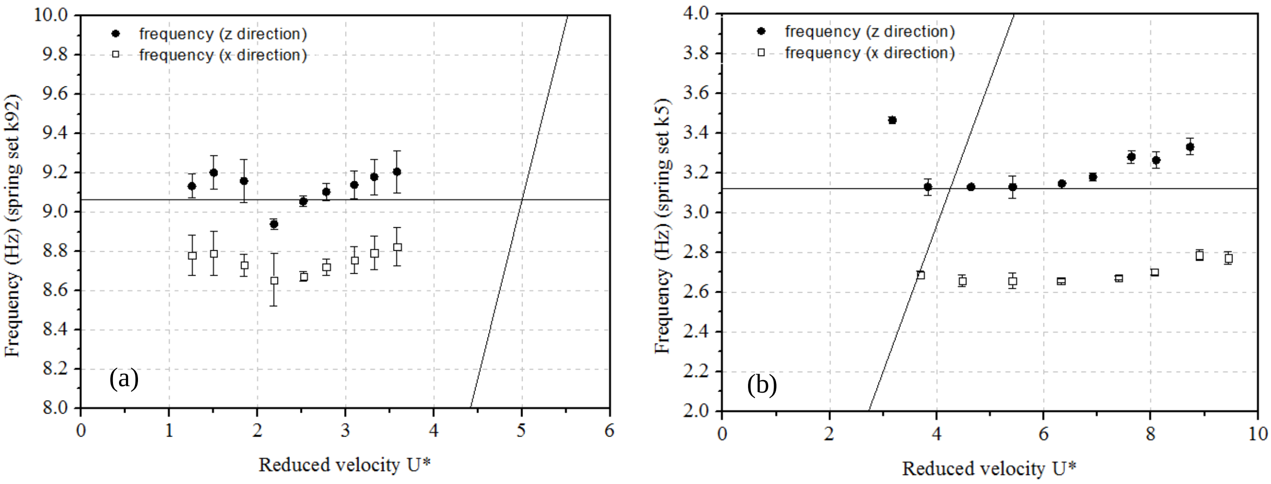

Figure 3. Reduced frequency comparison in both directions for spring sets (a) k92 and (b) k5.

The reduced frequency in the transversal direction presents a close behavior when compared with Assi (2005) data, whose data were obtained for a cylinder with mass ratio equal to 8.0. It can be noted that the vibration frequencies remain close to the cylinder's natural frequency, constituting a baseline close to unity for wide flow velocity, as can be seen in Figure 4.

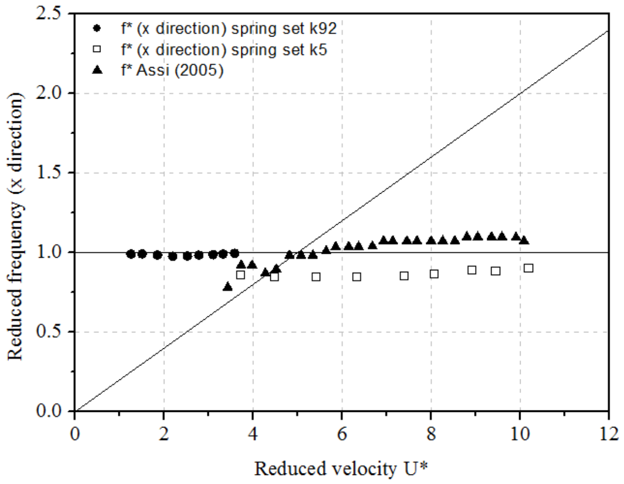

Figure 4.Comparison of reduced frequency data with literature.

3.2 Evaluation of the motion amplitudes

The motion amplitudes in the transversal direction are plotted against the reduced velocity in Figure 5. The markers represent the mean of the triplicate obtained via double integration of the acceleration signal and the error bars of the markers represent the standard deviation. Different response branches were obtained with both spring sets and the knowledge of the way that a structure transition from one branch to another is of great interest due to a significant change mainly in the oscillation amplitude.

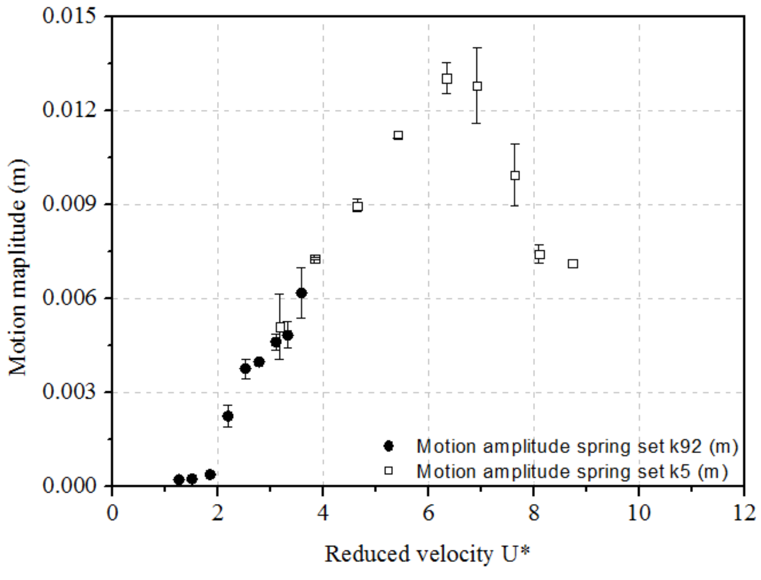

Figure 5. Motion amplitude comparison for both spring sets

The velocity range analyzed with spring set k5 includes the end of the initial excitation branch ($3.17 < U^* < 4.64$), the upper branch ($4.64 < U^* < 7.64$) and the beginning of the lower branch ($U^* > 8.00$). In the upper branch, although a not so evident transition from the initial branch can be noted, a gradual increase of the amplitude intensity takes place, reaching values up to 1.3D. According to Williamson and Roshko (1988), this branch develops a 2P vortex street, where a pair of vortices shed each half-cycle of oscillation, besides of a phase angle of 0º. From a reduced velocity of approximately 8, there is a second transition, reaching the lower branch, which is characterized by inferior oscillation amplitudes when compared to the upper branch. This branch develops a 2P vortex shedding pattern, however, the phase angle between the lift coefficient and the motion amplitude in the transversal direction is of 180º.

Analyzing the results obtained with spring set k92, only the initial branch can be observed, where there is an arising of the vibration amplitudes as the reduced velocity increases, reaching maximum values of 0.6D. On this branch, a 2S vortex shedding pattern can be observed, where a single vortex shed each half-cycle of oscillation, besides of a phase angle of 0º. In the lower velocities tested, the motion amplitude performed low standard deviations, close to 0.6%, while as the velocity increases, values showed greater variation in the experimental data acquired, obtaining maximum errors of 8.1%. In reduced velocities inferior to 1.85, almost no oscillation was observed, in a way that after this value, the initial excitation range soon develops. Although greater velocities were not practiced due to a limitation in the experimental facility, it can be noted a tendency of transition to the upper branch in the higher velocities tested. To determine this condition, experiments with higher velocities need to be conducted.

Comparing the responses obtained with both spring sets, there are few intersection points, as can be seen in Figure 5. In the common region for both spring sets, similar behavior can be observed, in a way that the oscillation amplitudes present close values.

Figure 6 presents the motion amplitudes dimensionless by the cylinder diameter for the experiments conducted in this work in comparison with literature data. Fujarra (2002) *apud* Assi (2005) conducted tests with a mass ratio $m^* = 10.0$ and a mass-damping parameter $m^*\zeta = 0.03$. Assi (2005) used a cylinder with $m^* = 8.0$ and $m^*\zeta = 0.014$. Khalak and Williamson (1999) used a tube with mass ratio equal to 10.3 and a mass-damping parameter of 0.017. The present work has a group cylinder-accelerometer with a mass ratio $m^* = 13.66$, a mass-damping parameter $m^*\zeta = 2.117$ for the spring set k5 and an $m^*\zeta = 0.085$ for spring set k92.

In a general overview, a similar behavior between the various tests can be noted in Figure 6. For reduced velocities below 2, no significant oscillations are observed for any data. However, the experiments conducted with spring sets k5 and k92 developed a wider response range when compared with other studies, evidencing greater vibration amplitudes for the same reduced velocity. In this context, an anticipation of the initial branch can be observed for the data acquired with spring set k92, besides of a higher amplitude peak in comparison with the other author's data and an upper branch with superior amplitudes.

Although greater amplitudes on the response peak are expected for inferior mass-damping parameters, the values obtained in this work contradicts this fact, once $m^*\zeta$ obtained with spring sets k5 and k92 are greater than the literature data. This explains the reason for Fujarra (2002) *apud* Assi (2005) data present a narrower response in comparison with Khalak and Williamson (1999) data, even with a similar mass ratio.

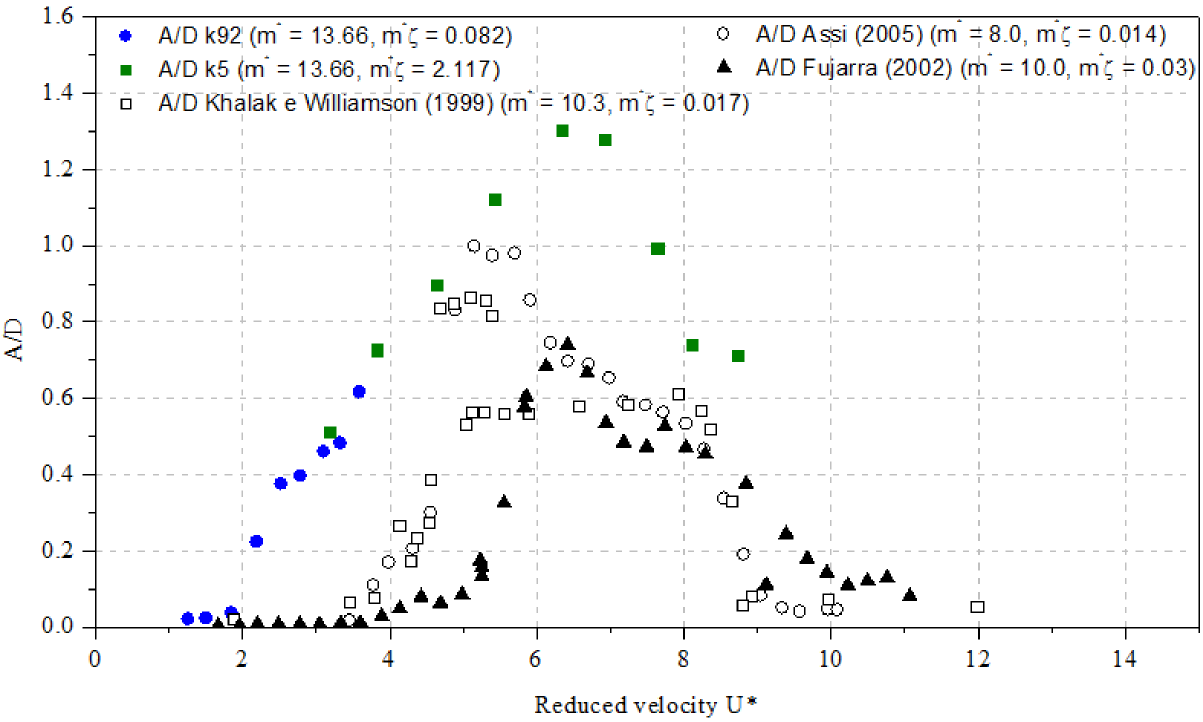

Figure 6. Comparison of the motion amplitude data with literature data

4. CONCLUSIONS

The study of the crossflow over bluff bodies is of great economic and industrial interests. Depending on the operating conditions employed, vibration can occur arising from the fluid-structure interaction, which can compromise the physical integrity of the equipments. The motion of the cylinder involves specific conditions of velocity and frequency to be reached, in such a way that the study of this subject includes the knowledge of some parameters that are essential for its categorization, such as mass ratio and natural vibration frequency. In the present study, amplitude and frequency responses of a single cylinder were experimentally investigated through accelerometry technique. The reduced frequency obtained from both spring sets performed a baseline close to the unity in both directions so that the oscillation frequency was close to the natural vibration frequency. The motion amplitude was characterized by an initial excitation branch with spring set k92, with the start of the synchronization and an abrupt increase in the displacement, while the upper branch and the beginning of the lower branch were achieved with the spring set k5. The responses developed an anticipated initial branch compared to other studies, with a rapid increase in the motion amplitude from a reduced velocity close to 2, compared with a U^* near 4 for other authors. Besides, a greater upper branch was visualized, reaching amplitude values up to 1.3 diameters.

5. ACKNOWLEDGMENTS

This study was financed by Coordenação de Aperfeiçoamento de Pessoal de Nível Superior – Brasil (CAPES) – Financial code 001. The authors would like to acknowledge the financial support from Petróleo Brasileiro S.A. (PETROBRAS) through the cooperation agreement 5850. 0103010.16.9.

6. REFERENCES

Assi, G.R.S., 2005. *Estudo experimental do efeito de interferência no escoamento ao redor de corpos alinhados*. Master dissertation, Escola Politécnica da Universidade de São Paulo, São Paulo, Brasil.

Barbieri, M.R., Silva, B.L., Utzig, J. and Meier, H.F., 2018. "CFD-based study of flow-induced vibrations in cylinder arrays with air as working fluid". In *Proceedings of the 11th ABCM Spring School on Transition and Turbulence – EPTT 2018.* Uberlândia, Brazil.

Bearman, P.W., 2011. "Circular cylinder wakes and vortex-induced vibrations". *Journal of Fluids and Structures*, Vol. 27, pp. 648-658.

Blevins, R.D., 1990. *Flow-Induced Vibration*. Van Nostrand Reinhold, New York, 2nd edition.

Goyder, H.G.D., 2002. "Flow-Induced Vibration in Heat Exchangers". *Chemical Engineering Research and Design*, Vol. 80, pp. 226-232.

Jauvtis, N. and Williamson, C.H.K., 2004. "The effect of two degrees of freedom on vortex-induced vibration at low mass damping". *Journal of Fluid Mechanics*, Vol. 509, pp. 23-62.

Khalak, A. and Williamson, C.H.K., 1997. "Investigation of relative effects of mass and damping in vortex-induced vibration of a circular cylinder". *Journal of Wind Engineering and Industrial Aerodynamics*, Vol. 69-71, pp. 341-350.

Khalak, A. and Williamson, C.H.K., 1999. "Motion, forces and mode transitions in vortex-induced vibrations at low mass-damping". *Journal of Fluids and Structures*, Vol. 13, pp. 813-851.

Norberg, C., 2003. "Fluctuating lift on a circular cylinder: review and new measurements". *Journal of Fluids and Structures*, Vol. 17, pp. 57-96.

Silva, B.L., Luciano, R.D., Utzig, J. and Meier, H.F., 2019. "Analysis of flow behavior and fluid forces in large cylinder bundles by numerical simulations". *International Journal of Heat and Fluid Flow*, Vol. 75, pp. 209-226.

Silva, B.L., Luciano, R.D., Utzig, J. and Meier, H.F., 2018. "Flow patterns and turbulence effect in large cylinder arrays". *International Journal of Heat and Fluid Flow*, Vol. 69, pp. 136-149.

Silva, B.L., Utzig, J. and Meier, H.F., 2016. "CFD-based design of experiments for the study of flow-induced vibrations in a tube bundle". In *Proceedings of the 10th ABCM Spring School on Transition and Turbulence – EPTT 2016*. São José dos Campos, Brazil.

Vikestad, K., Vandiver, J.K., Larsen, C.M., 2000. "Added mass and oscillatory frequency for a circular cylinder subject to vortex-induced vibration and external disturbance". *Journal of Fluids and Structures*, Vol. 14, pp. 1071-1088.

Williamson, C.H.K. and Govardhan, R., 2008. "A brief review of recent results in vortex-induced vibrations". *Journal of Wind Engineering and Industrial Aerodynamics*, Vol. 96, pp. 713-735.

Williamson, C.H.K. and Roshko, A., 1988. "Vortex formation in the wake of an oscillating cylinder". *Journal of Fluids and Structures*, Vol. 2, pp. 355-381.

7. RESPONSIBILITY NOTICE

The authors are the only responsible for the printed material included in this paper.